JOURNAL OF CATALYSIS 45, 54–67 (1976)

Catalysis-Inhibition Effects of Oxidized Copper Surfaces in the Autoxidation of Hexadecane

The Role of Copper–Oxygen Surface Species

D. L. ALLARA AND R. F. ROBERTS

Bell Laboratories, Murray Hill, New Jersey 07974

Received April 30, 1976

The reaction of hexadecane with oxygen at 100°C over oxidized copper surfaces has been studied. The reactions were initiated by added *t*-butyl hydroperoxide. For air-aged copper powder critical concentrations of added hydroperoxide exist, below which the oxidations are almost totally inhibited and above which catalysis is quite marked. Based on kinetic and X-ray photoelectron spectroscopic data, it appears that the critical concentration phenomenon is due to different types of surface reactions of hydroperoxides on each of several different copper–oxygen surface species.

INTRODUCTION

The oxidation of hydrocarbon materials over copper/copper oxide surfaces is an area of considerable practical interest. Significant examples are the gas-phase conversion of propylene to acrolein (*1*) at around 300°C and the catalyzed oxidations of various liquid-phase hydrocarbons and solid-phase polyolefins (*2*) over copper/copper oxide surfaces at near, or slightly above, ambient temperatures. The latter, low-temperature reactions, have been the subject of very few fundamental studies, in contrast to the former. The oxidation of polyethylene in contact with copper below 90°C has given some details of the polymer-interface chemistry (*3*). Few mechanistic details can be determined because of obvious experimental difficulties in such solid phase systems. Liquid- or gas-phase hydrocarbon systems are much more amenable to a fundamental approach and two apparently conflicting studies have been reported on the oxidation of cumene over copper. Casemier, Nieuwenhuys, and Sachtler (*4*) observed no catalytic effect of copper at 90–100°C. In contrast, Shalya and coworkers (*5*) reported significant catalytic effects in the cumene/copper system at 60–90°C. A possible factor in this discrepancy could be that different surface structures exist on the copper since each group used different preparative methods. A study of the oxidation of several hydrocarbons over copper at 90–100°C has been reported by Poling (*6*). The copper samples (optically flat plates) were characterized by reflection infrared spectroscopy. In the case of decane oxidation, Poling speculated that surface-catalyzed hydroperoxide decomposition accounts for the appearance of various observed carboxylate surface species. However, these data do not yield much information on the detailed nature of the catalytic processes in the early stages of reaction, and furthermore, it is not clear how effectively the copper surfaces control the major course of the oxidations since the effective surface area of the

copper plates is extremely small compared to typical catalytic reactions.

At the low temperatures of these preceding studies, the surface oxide film covering the copper metal generally would be expected to be Cu_2O, as Poling (*6*) observed, and thus one would expect that this metal oxide is the actual catalyst of concern. Two fundamental studies have been made over bulk oxide catalysts. Mukherjee and Graydon (*7*) have studied the kinetics and products of the oxidation of tetralin at 45–90°C over Cu_2O as well as several other metallic oxides. In addition, these authors reported the interesting observation that below a critical ratio of hydroperoxide concentration to catalyst weight, no oxidation will begin over Mn_2O_3, and they suggest a similar phenomenon for Cu_2O. Gould and Rado (*8*) have studied the oxidation of cyclohexene over bulk CuO at 70°C. Both of the above groups conclude that oxidation proceeds by a free-radical chain route with surface initiation processes: hydroperoxide decomposition (*7*, *8*) and a direct free-radical forming reaction with substrate hydrocarbon (*8*).

There are two major obstacles in comparing and interpreting the above studies. First, the actual surface areas of the catalysts were not reported. Secondly, and perhaps ultimately the more important, the exact nature of the surface species of the catalysts was not defined. It is clear that one should expect a very close relationship between overall catalytic effects and the type of metal oxide surface species present when the initial adsorption reactions occur. Studies of chemisorption reactions of azoles on various copper oxide surfaces (*9*) have shown that the chemical reactivity of the surface can be quite dependent on the oxidation state of the copper surface species. Of particular relevance is a recent study by Robert, Bartel, and Offergeld (*10*) in which the detailed nature of various copper oxide surfaces was examined by X-ray photoelectron spectroscopy. This study defines the existence of four types of copper oxide surface species and shows that the predominant species residing on a Cu_2O film is determined by the type of film pretreatment with respect to variables such as temperature, O_2, and water vapor.

The present study was undertaken to elucidate some details of the mechanism(s) of the oxidation of a simple liquid-phase alkane over copper/copper oxide surfaces. Hexadecane, n-$C_{16}H_{34}$, was chosen as the alkane because of the presence of essentially only one type of C–H bond (a secondary C–H) and because of its low vapor pressure. The copper used was in the form of powders in order to attain high surface areas. Such a choice, unfortunately, also precluded the use of a variety of spectroscopic techniques to study the surfaces. However, the surfaces of a limited number of the copper powders were examined by X-ray photoelectron spectroscopy (XPS). The kinetics of oxidation were followed by oxygen absorption, and extensive attempts were made to use catalysts where both the chemical state of the copper oxide surface species and the overall surface area were known. Conversions were kept low (<0.1%) to ensure minimum secondary oxidation of products, and *t*-butyl hydroperoxide was added in known amounts to initiate the oxidations under controlled conditions. The existence of a "critical" hydroperoxide/catalyst concentration, as suggested by Mukherjee and Graydon (*7*) for tetralin, was examined carefully in hopes that the phenomenon, if present, could be correlated with catalyst surface structure.

EXPERIMENTAL

Materials

The *t*-butyl hydroperoxide was obtained from the Lucidol Division of Pennwalt. Iodometric titration (*11*) showed it to be 97% pure; the impurities were *t*-butyl alcohol and water. It was added to the

reactions as a solution in decane. Hexadecane (>99.9% purity) and decane (>99.9% purity) were obtained from the Chemical Samples Company and were stored under nitrogen. Prior to each use these alkanes were passed through a column of alumina, Grade 2, to remove any traces of residual hydroperoxides. Copper powder of purity >99.9% was obtained from Alfa Inorganics. It was passed through 20–40 μm sieves to remove any large particles and then heated to 310°C *in vacuo* ($\sim 10^{-5}$ Torr) in a glass chamber closed off at both ends by coarse fritted glass discs. Hydrogen gas was admitted to a pressure of $\sim$1 atm for 30 min. The gas was allowed to flow through the sample by alternately pumping and charging the reactor chamber several times. The chamber was evacuated and cooled *in vacuo* ($\sim 10^{-6}$ Torr). The sample was then stored in air. These samples are referred to as the standard copper/air catalysts and were used as the basic starting materials for preparation of the various types of copper oxide surfaces described in the text. The CuO was obtained from Matheson, Coleman, and Bell as the reagent grade powder and was subjected to extensive degassing to remove adsorbed volatile impurities.

Surface Characterizations

The surface areas were measured by the BET method using both N_2 and Kr gases. X-ray photoelectron spectra were recorded with a Varian VIEE-15 induced electron emission spectrometer system using Mg$K\alpha$ (1253.6 eV) radiation as the excitation source. During measurements the pressure and temperature in the spectrometer were $\lesssim 10^{-7}$ Torr and $\sim$35°C, respectively. In order to minimize reduction of cupric species in the spectrometer (*9*), spectra were accumulated in the minimum time required to give good count rates. The copper powders were stored under argon prior to XPS measurement. Spectra were obtained by thinly spreading the copper powders onto Scotch double-coated tape which was mounted on cylindrical aluminum sample holders. The C(1*s*) signal at 285.0 ± 0.2 eV from minor vacuum pump oil contamination was used to correct the spectra of the powders for sample charging.

Kinetics

Apparatus. In all cases the reaction rates were followed by the decrease in the oxygen pressure above the hexadecane reaction solution. An MKS Baratron 0–100 Torr differential pressure transducer was connected to the reaction flask and a stainless steel reference pressure chamber. The pressure system, including valve bodies and connecting tubing but excluding the transducer head, was completely immersed in the constant temperature bath (100.0 ± 0.01°C) and connected to an external gas-vacuum manifold at ambient temperature. The transducer head was maintained internally at 50°C. The reactor vessel was connected to the transducer measurement port with an 18-in. flexible stainless steel bellows hose using a stainless steel swagelok fitting. All other tubing in the system was copper, and all joint connections were done by sweat-soldering. The output of the transducer was fed into a strip chart recorder and/or an Esterline–Angus digital data acquisition system with printed and paper tape output. The transducer range was normally set to 10 Torr full scale. Signal excursions due to temperature cycling of the temperature bath could not be detected in this pressure range. The volume of the measurement side of the transducer was calibrated using known volume calibration vessels and the ideal gas law. The volume measurement was reproducible to ±0.5%. The glass reactor vessels were constructed as a spherical bulb attached to cylindrical neck equipped with a glass–metal seal side arm. The flask was made as two separate halves with O-ring joint grooves and thus was assembled using an

O-ring and a screw clamp. A small charge of Type 3A Linde molecular sieve was placed in the vessel neck between the side arm and a coarse fritted glass disc located in the lower part of the vessel neck. The molecular sieve was used to trap small amounts of water vapor, CO, and CO_2 which could form.

Procedures. A typical run was conducted as follows. Hexadecane and hydroperoxide solution were added to a reaction flask bottom piece of known volume containing a weighed amount of catalyst. In cases where the catalyst underwent a pretreatment, the latter was carried out directly in the reactor flask, and the reactor was then filled with argon until final use. The flask top and bottom were assembled with the O-ring and clamp and connected to the transducer. With the transducer bypass valve open the reactor was evacuated to ~0.2 Torr and filled with O_2 twice at ambient temperature. The vessel was then completely immersed in the temperature bath and evacuated and filled with O_2 again to be a fixed pressure measured with a Pennwalt mechanical precision pressure gauge. The reference chamber and the bypass valve were closed to isolate the pressure system and the reactor vessel agitated using a Burrell wrist-action shaker. Approximately 30 min were required for the reactor system to come to complete pressure equilibrium as detected by the transducer in the sensitive 0–10 Torr differential range. This time could be reduced considerably by a thorough outgassing of the reaction system with a blank vessel after every run. Corrections for the changes were made in the final pressure–time curves by ignoring early time fluctuations (<30 min) and by subtracting control curves, generated by blank reactions, for later times. The pressure drops were converted to moles of oxygen consumed using the known reactor and measurement system volumes and the ideal gas law. For a typical reactor flask 1 Torr of ΔP is approximately 8×10^{-6} mol of ΔO_2. Whenever the pressure drop exceeded 10 Torr, the transducer bypass valve was opened, the reference and reaction arm reequilibrated, and the bypass valve again closed. Thus, the total O_2 pressure was always constant to within 10 Torr. At 700 Torr total pressure, for example, this amounts to 1.4% variation. After reaction the solutions were decanted from the catalysts and stored in stoppered vials in a freezer. The hydroperoxide content of selected solutions were determined using the Hiatt (*11*) method. In some cases the catalysts were washed with pure hexane several times, dried *in vacuo*, and stored under argon for analysis by X-ray photoelectron spectroscopy.

RESULTS

Standard Air-Aged Catalyst Runs

One batch of aged copper powder prepared in the standard way was used for an entire series of runs in which rate behavior was studied as a function of catalyst surface area and initial *t*-butyl hydroperoxide concentration. The Cu(2*p*) and O(1*s*) XPS spectrum of a sample of the standard air-aged copper powder, prior to these experiments, is shown in Fig. 1(a). The binding energies of the Cu($2p_{\frac{3}{2}}$) and Cu($2p_{\frac{1}{2}}$) signals and the existence of satellites (9) indicate that Cu^{2+} resides in the surface region of this catalyst. The broadness of the O(1*s*) peak suggests the presence of two oxygen species: the major component at 529.9 eV is attributable to lattice oxygen (*9*), O^{2-}, while the higher-binding-energy component is consistent with the presence of OH^- (*10*). All kinetic runs were carried out at a constant pressure of oxygen of 700 Torr at the standard temperature of 100.0°C. Selected, representative curves are given in Figs. 2–4 for average values of catalyst surface area concentrations of 6.8×10^{-2}, 1.7×10^{-2}, and 4.3×10^{-3} m^2/g of solution, respec-

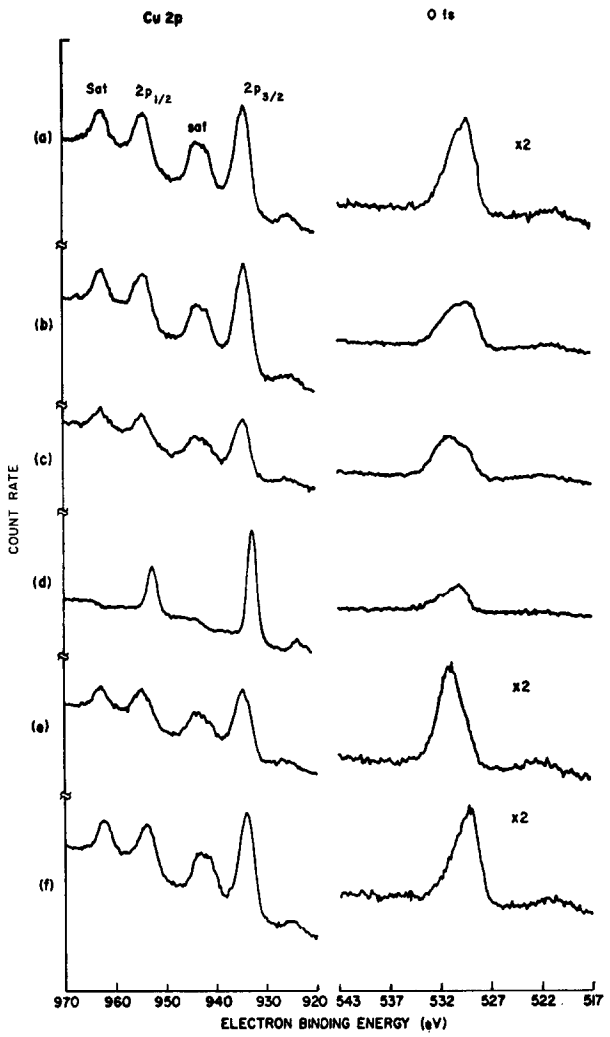

FIG. 1. Copper ($2p$) and oxygen ($1s$) XPS spectra: (a) standard air-aged copper powder; (b) standard air-aged copper powder after 60 h (50 μmol of O_2 absorbed) inhibited run with no added hydroperoxide; (c) standard air-aged copper powder after 6.5 h ($\sim$100 μmol of O_2 absorbed) inhibited run with 4.0×10^{-4} m initial hydroperoxide; (d) Cu_2O generated by immersion of standard air-aged copper in dilute aqueous HNO_3; (e) Cu_2O after 48 h reaction in oxidizing hexadecane; (f) CuO prior to use in an oxidation.

tively. In Fig. 5, selected representative curves are given for control experiments with no added catalyst. A synopsis of most of these experiments is given in Table 1. Several interesting features of these experiments are immediately obvious: (i) For each catalyst surface area there exist two types of rate behavior: one displaying a very fast rate above a critical concentration range of the initial t-butyl hydroperoxide, and one displaying a very much slower rate below this critical concentration range. (ii) These critical concentrations are sensitive functions of the catalyst surface area. (iii) Comparison of Fig. 5 with the other figures shows that the fast type of rate involves strong acceleration of the normal autoxidation process, while the slow rate

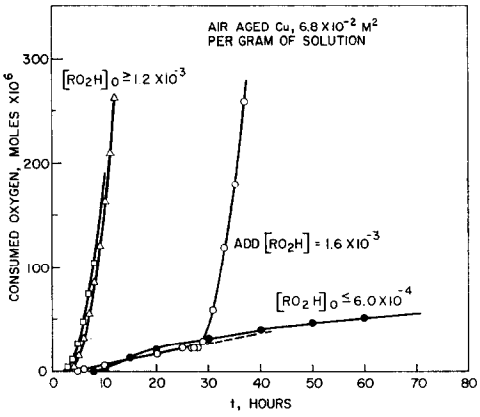

FIG. 2. Oxidation of hexadecane over standard air-aged copper; average surface area per gram of solution = 6.8×10^{-2} m²; initial [t-BuO_2H] molal: △, 1.75×10^{-3}; □, 1.20×10^{-3}; ○, 6.0×10^{-4} (1.6×10^{-3}); ●, 3.4×10^{-4}.

mode involves a corresponding rate depression. These effects are quite pronounced at high surface areas, 6.8 and 1.7×10^{-2} m²/g of solution (Figs. 2 and 3); but at the lower surface area, 0.43 m²/g of solution, there is almost no catalysis effect, although the inhibition is fairly pronounced (Fig. 4). The relationship between the critical range of the initial hydroperoxide and the

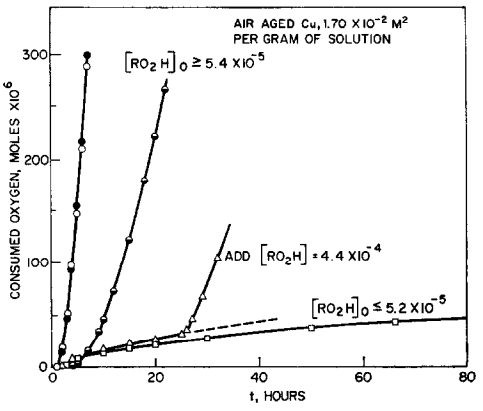

FIG. 3. Oxidation of hexadecane over standard air-aged copper; average surface area per gram of solution = 1.70×10^{-2} m²; initial [t-BuO_2H], molal: ○, 1.34×10^{-4}; ●, 5.41×10^{-5}; □, 5.20×10^{-5}; △, ○ (4.4×10^{-4}); ◒, 9.48×10^{-5} ([t-BuOH] = 2.0×10^{-4}).

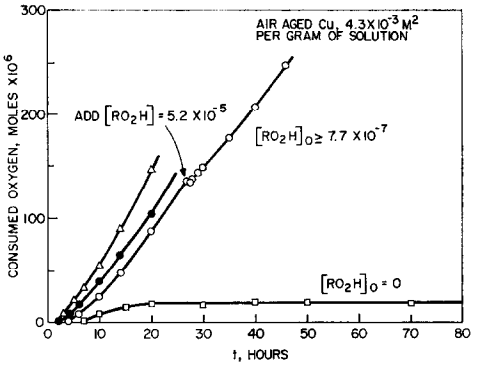

FIG. 4. Oxidation of hexadecane over standard air-aged copper; average surface area per gram of solution = 4.3×10^{-3} m²; initial [t-BuO_2H], molal: ○, 2.8×10^{-5} (5.2×10^{-5}); ●, 5.7×10^{-2}; △, 7.7×10^{-7}; □, 0.

catalyst surface area (σ in m²/g of solution) is given in Fig. 6 where the error bars indicate the magnitudes of the critical ranges. For the middle point (1.7×10^{-2}) the range was too small for this notation. No lower critical concentration range was determined, but an upper limit of 7.7×10^{-7} m was observed. At the two higher concentrations the approximate relation can be written:

$$[t\text{-}BuO_2H]_{critical} \propto \sigma^2.$$

Two runs which were in the inhibition mode were interrupted and injections of t-butyl hydroperoxide made in sufficient amounts

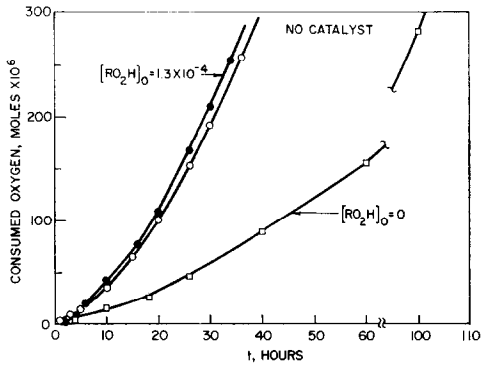

FIG. 5. Oxidation of hexadecane (catalyst-free); initial [t-BuO_2H], molal: ○, 1.30×10^{-4}; ●, 4.1×10^{-5}; □, 0.

TABLE 1

Oxidation of Hexadecane over Variously Pretreated Cu Powder Samples Conditions: 100.0°C, 700 Torr O_2

Sample and pretreatment	Run	Surface area of catalyst per gram of solution ($m^2 \times 10^2$)	$[t\text{-}BuO_2H]_0$ molal	Result[a]
Standard Cu powder	6-97	7.0	1.75×10^{-3}	cat
reduced in H_2 at 310°C	6-98	6.8	1.20×10^{-3}	cat
and aged in air under	6-38	6.6	6.0×10^{-4}	inh
ambient conditions,	6-36	6.7	3.4×10^{-4}	inh
designated as Cu (air)	6-11	6.2	9.4×10^{-5}	inh
sample	5-55	1.71	1.34×10^{-4}	cat
	5-57	1.71	6.75×10^{-5}	cat
	5-60	1.73	5.41×10^{-5}	cat
	5-75	1.70	5.20×10^{-5}	inh
	5-61	1.73	3.98×10^{-5}	inh
	6-32	1.72	0	inh
	6-14	0.43	2.8×10^{-5}	ne
	6-16	0.42	5.7×10^{-6}	ne
	7-22	0.44	1.93×10^{-6}	ne
	7-25	0.43	7.7×10^{-7}	ne
	6-45	0.43	0	in
Cu (air) sample annealed	7-18[b]	1.66	1.67×10^{-3}	part. inh
at 280°C/10^{-5}–10^{-7} Torr	7-15	1.67	1.00×10^{-3}	cat
3 h, designated as	6-70	1.73	3.0×10^{-4}	inh
Cu (air)-annealed sample	7-16	1.72	8.4×10^{-5}	inh
Cu (air) sample treated with 0.1 *M* HNO_3	6-8	1.70	4.0×10^{-4}	part. inh
Cu (air)-annealed sample	7-19[b]	1.71	7.9×10^{-3}	cat
oxidized in O_2/H_2O several	7-36[b]	1.72	4.0×10^{-3}	inh
days	7-31[b]	1.71	1.04×10^{-4}	inh
	7-17	1.66	8.0×10^{-4}	inh
	6-78	1.73	3.2×10^{-4}	inh
	6-67	1.73	6.1×10^{-6}	inh
Cu (air)-annealed sample	7-30[b]	1.72	2.2×10^{-3}	part. inh
oxidized in dry O_2 several	7-29[b]	1.73	5.5×10^{-4}	part. inh
days				
Bulk CuO	5-97	1.84	4.6×10^{-4}	cat
	6-73	1.70	0	cat

[a] cat = catalysis; inh = inhibition; part. inh = partial inhibition; ne = no effect.
[b] Samples were reduced in CO for 30 min at 140°C after annealing.

to raise the concentrations to greater than the critical limit. In both cases, shown in Figs. 2 and 3, the reactions almost immediately switched to the catalysis mode.

The critical points are also a function of the type of exposure undergone on catalyst aging. Several runs at random conditions were made with different copper powder,

prepared in the standard way, but aged in different containers with differing exposure to ambient conditions. The critical concentration ranges definitely were observed but were shifted within one or two orders of magnitude of those observed in Fig. 6 with the primary experimental batch.

Two types of experiments were performed to ascertain whether the influence of the catalyst on these oxidations occurred only through heterogeneous surface reactions. Both types of experiments described below gave no evidence for a significant homogeneous component. Typical runs in the catalysis and inhibition modes were interrupted, the catalyst removed by centrifuging, the supernatant solution quickly placed back into the reactor, and the typical reaction conditions reestablished. The results are shown in Fig. 7, where it can be seen that in both cases an autocatalytic oxidation ensues with a curve shape

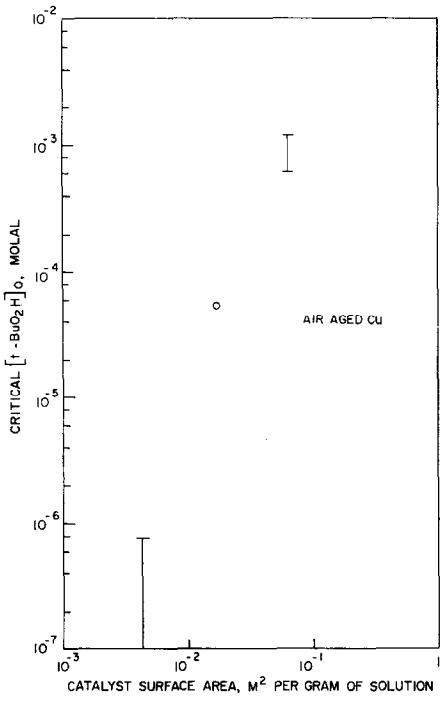

FIG. 6. Relationship between critical [t-BuO_2H] ranges and catalyst surface area for oxidation of hexadecane over standard air-aged copper.

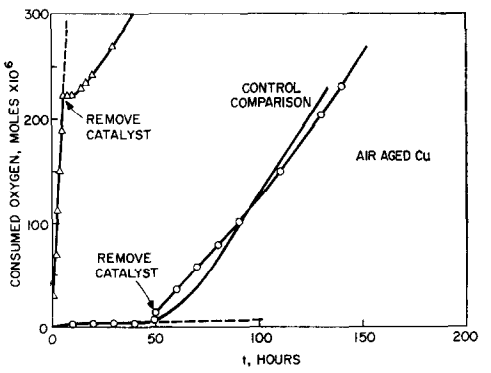

FIG. 7. Oxidation of hexadecane over standard air-aged copper; △, accelerated run, catalyst removed at 6 h; ○, in inhibited run, catalyst removed at 49 h; —, control run, no catalyst.

similar to that for the oxidation of pure hexadecane (run 7–72, from Fig. 5). As regards the accelerated, catalytic mode, any homogeneous catalysis which might occur would be expected to arise from dissolution of copper oxide by organic carboxylic acids to yield ultimately cupric carboxylate salts (*12*, *13*). Hence, if the catalytic effects were homogeneous in nature, addition of a carboxylic acid to a reaction solution should enhance these effects. Experiments were performed with hexadecane solutions containing $\sim 5 \times 10^{-4}$ m t-butyl hydroperoxide, catalyst with surface area of $\sim 7.0 \times 10^{-2}$ m^2/g of solution, and octanoic acid in concentrations of 3.3×10^{-5}, 1.7×10^{-4}, and 8.4×10^{-4} m. Without the added acid the rates would have been of the accelerated mode, as in Fig. 3. However, the octanoic acid runs showed less accelerated rates (about one-third as large) and zero induction times with the highest acid concentration giving the fastest initial rates. The solutions also developed weak blue coloration after several hundred micromoles of oxygen were consumed, which indicates solubilization of cupric salts. Thus the addition of the acids did not enhance the catalytic effects even though catalyst solubilization had occurred. It is interesting

TABLE 2

Total Hydroperoxide Yields for the Autoxidation of Hexadecane at 100°C

Run	Catalyst	Catalyst surface area, m^2/g of solution, $\times 10^2$	Initial [t-BuO_2H], molal	ΔO_2, moles $\times 10^6$	Moles consumed O_2 per 100 mol CH_2 groups	Final [RO_2H], molal	$\Delta RO_2H/\Delta O_2 \times 100$
5-72	—	—	0	518	0.091	0.054	90
5-56	—	—	1.3×10^{-4}	392	0.067	0.034	77
5-74	—	—	2.5×10^{-4}	484	0.084	0.044	78
5-49	—	—	1.2×10^{-3}	633	0.11	0.050	69
6-86	Cu(air)	0.13	1.1×10^{-4}	~1100	~0.19	0.091	~72
6-16	Cu(air)	0.42	5.7×10^{-6}	112	0.020	0.012	91
6-77	Cu(air)	1.66	9.5×10^{-5}	266	0.044	0.015	49
6-98	Cu(air)	6.8	1.2×10^{-3}	~ 800	~0.14	0.041	~46
6-97	Cu(air)	7.0	1.8×10^{-3}	~1250	~0.22	0.052	~36
6-73	CuO	1.70	0	270	0.046	0.022	71
5-97	CuO	1.84	4.6×10^{-4}	683	0.13	0.037	44

to) note that when normal (no added acid oxidations with copper powder were carried to high conversions (several thousand micromoles of O_2 consumed), the solutions often developed weak blue–green colors, which indicates that solubilization of the catalyst was occurring.

The qualitative nature of the products was examined. The yields of total hydroperoxide were determined by titration and are given in Table 2. The average yields of total hydroperoxide for runs under a variety of conditions are around 40–90% of the consumed oxygen when a catalyst is present and 70–90% for catalyst-free runs. The remainder of the products are expected to be mostly carbonyl products, predominantly aldehydes and alcohols. Infrared spectra of typical product solutions [for Cu(air) catalyst] show the expected broad carbonyl absorption at 1715 cm^{-1}, which indicates the presence of aliphatic aldehydes, carboxylic acids, and ketones. Other bands were too weak to enable reasonable assignments.

The stability of the initial catalyst surface species composition during an oxidation was examined in two cases. In one inhibited run with no added hydroperoxide, after 60 h (50 μmol of O_2 absorbed) the catalyst was collected in the usual way and its XPS spectrum taken. The spectrum is shown in Fig. 1(b) and is essentially identical to that of the standard air-aged copper powder [Fig. 1(a)], which is consistent with the presence of Cu^{2+}, O^{2-}, and OH^- in the surface region of this sample. In another run with 4.0×10^{-4} m initial hydroperoxide, which exhibited strong catalysis, the catalyst was removed in the usual way after 6.5 h (~100 μmol of O_2 absorbed) and the XPS spectrum obtained. Except for a reduction in the intensity of the signals, the Cu(2p) spectrum of this sample [Fig. 1(c)] is essentially the same as that obtained for the sample of the previous inhibition run. The broad asymmetric O(1s) peak [Fig. 1(c)], however, now has a major component at 531.3 eV which is attributable to OH^- (*10*), while the lower-binding-energy component is consistent with the presence of O^{2-}. Both of these experiments suggest that no major changes in the surface structure of the copper (air) catalyst occur during the low conversion stages of the oxidation. Further, the results must be viewed cautiously, as it is not clear whether small changes might be

induced in the catalyst by the solvent washing and drying procedures.

Since the results indicated a direct reaction of hydroperoxides with the copper surfaces, it was of interest to know some details about the adsorption process for hydroperoxides. An adsorption isotherm was determined for a hexadecane solution of *t*-butyl alcohol, an approximate and unreactive model for *t*-butyl hydroperoxide, at 25°C over the Cu(air) surface. The amount of the adsorbed alcohol was determined from gas-phase chromatographic measurements on a Carbowax 20-M column. In a plot of adsorbed alcohol against actual alcohol concentration in solution, the data points had considerable scatter, but there appeared to be a discernible step at around 1×10^{-4} mmol/m^2 of catalyst (BET area), and the adsorption flattened out to a final value of $\sim 3 \times 10^{-3}$ mmol/m^2 of catalyst. These values correspond to each alcohol group occupying a site of dimensions $\sim 7 \times 7$ Å for the major site and the presence of $\sim 3\%$ of a site more strongly adsorbing than the major site. Such results are to be considered as qualitative, in view of experimental errors and the assumption that the *t*-butyl alcohol is a valid model for the hydroperoxide.

Other Types of Copper Oxide Surfaces

In order to examine the catalytic effects of chemical alternations of the copper surface structure, it was necessary to prepare surfaces in which the major chemical features were known. In this study the methods of preparation of Robert, Bartel, and Offergeld (*10*) were followed. The various surfaces, their methods of preparation, and their catalytic effects are described below. From control experiments there appeared to be no significant change of catalyst surface area (BET) by the pretreatment procedures. All copper samples were individually pretreated directly in the autoxidation reactor flask, starting with the air-aged material, and used immediately thereafter or stored briefly under argon. The results of kinetic runs are shown in Table 1. All the runs below were made with catalyst surface areas of $\sim 1.7 \times 10^{-2}$ m^2/g of solution, and the results thus can be compared directly with runs 5-55, -57, -60, -75, and -61 of the standard Cu(air) catalyst.

Annealing a copper oxide surface at 280°C for 3 h at 10^{-7} Torr is reported (*10*) to convert cupric species to cuprous species. Standard Cu(air) samples were pretreated thusly, and their catalytic effects are given in Table 1 for runs 7-15, 6-70, and 7-16. Comparison with the standard Cu(air) runs at the same surface area shows that a somewhat higher initial concentration of hydroperoxide ($\sim$ factor of 10) is required for the onset of the catalysis mode when the curpric sites are removed initially.

Oxidation of a copper surface with pure O_2 at low temperatures (near ambient) is reported (*10*) to convert a Cu_2O surface to one with a chemisorbed O species having less negative charge than O^{2-}. The kinetic results for dry O_2 oxidation of a preannealed Cu(air) sample are given in Table 1 for runs 6-65 and -66. The effect of increasing the chemisorbed O species in the standard Cu(air) surface is seen to be a small increase in the initial hydroperoxide required for onset of the catalysis mode.

Oxidation of a surface of Cu_2O species with O_2 saturated with water at ambient temperatures produces a cupric hydroxide species (*10*). Runs 7-17, 6-78, and 6-67 in Table 1 show that an increase of the cupric hydroxide species in an annealed Cu(air) surface results in substantial increase in the initial hydroperoxide required for onset of the catalysis mode.

Several runs were made in which a surface of pure Cu_2O was prepared and used directly or converted to another type of surface. These experiments avoided starting with a mixture of surface species as we propose exists in the Cu(air) samples. Reduction of a copper oxide surface at

140°C with several Torr of CO produces a nearly pure Cu_2O surface (*10*) in Run 7-18 (Table 1 and Fig. 6) it is observed that such a surface is catalytically inactive even at $[t\text{-}BuO_2H]_0 = 1.67 \times 10^{-3}$ *m* [~50 times the critical concentration for the standard Cu(air) sample] and in fact exhibits an ability to inhibit the normal oxidation of a catalyst-free run. Such an inhibition is not quite as pronounced initially as in the typical inhibition mode of other runs in Table 1, but even after 100 h reaction the rate is definitely inhibited (compare with Figs. 2–4). A Cu_2O surface was also prepared by immersing the standard Cu(air) catalyst in dilute aqueous nitric acid, rinsing the material in distilled water, and finally drying it *in vacuo*. The Cu(2*p*) and O(1*s*) XPS spectra of a sample treated in this manner are shown in Fig. 1(d). The binding energies of the Cu(2*p*) signals, their reduced widths, the absence of satellites, and the 530.6 eV binding energy of the major O(1*s*) component all confirm (*9*, *10*) the existence of an essentially pure Cu_2O surface region on this sample, although a minor amount of OH^- may be present. The oxidation rate behavior, using this essentially pure Cu_2O sample, is nearly identical to that of the previous run (compare runs 6-8 and 7-18 in Table 1). Removal of this catalyst after 48 h and examination with XPS indicated [Fig. 1(e)] that the initial Cu_2O surface species had been substantially converted to a Cu^{2+} species as indicated by Cu(2*p*) electron binding energies and the presence of satellites. Furthermore, the O(1*s*) signal at 531.5 eV is consistent with the presence of a predominant amount of OH^-, although its width allows for the presence of a minor amount of other oxygen species. Several standard Cu(air) samples were prereduced in CO and then subsequently oxidized in H_2O-saturated O_2 at ambient temperature (for at least six days) to give a surface which would be predominantly covered by $Cu(OH)_2$ species (*10*). Runs 7-19 and -31 show that this surface is strongly inhibiting but ultimately becomes catalytic at $[t\text{-}BuO_2H] \geq 7.9 \times 10^{-3}$ *m* [>100 times the critical concentration for the Cu(air) sample].

Finally, a series of runs were made using as-received CuO, whose XPS spectrum is shown in Fig. 1(f). The Cu(2*p*) electron binding energies and satellites confirm the presence of Cu^{2+} in the surface retion of this catalyst, while the major O(1*s*) component at 529.9 eV is attributable to O^{2-}. The higher-binding-energy component of the broad O(1*s*) peak is consistent with the presence of some OH^-. At $[t\text{-}BuO_2H]_0 = 4.55 \times 10^{-4}$ *m* ,the oxidation exhibited zero induction time, compared to 1 to 3 h for the other copper forms, but otherwise exhibited the characteristics of the normal catalysis mode. At $[t\text{-}BuO_2H]_0 = 0$, an induction time of several hours was observed, followed by a normal catalysis mode. Thus, CuO behaves catalytically at all hydroperoxide concentrations of added hydroperoxide.

DISCUSSION

The present results clearly establish a sharp dichotomy in the catalytic behavior of an air-aged Cu surface with the mode of behavior a function of initial hydroperoxide concentration. The type of effect observed is definitely a function of the initial copper and oxygen surface species on the copper catalyst, and these effects are briefly summarized in Table 3. The results are interpreted in terms of surface-catalyzed decompositions of hydroperoxides. Proposed generalized reaction paths for the latter are given in Table 3 and are discussed below in detail.

The catalyst-free autoxidation of hexadecane at 100°C can be thoroughly understood in terms of well-known free-radical reactions. Detailed mechanisms have been derived for the oxidation of alkane molecules (*14–19*), and the following can be considered as the major contributing types of reactions to the overall process at low

TABLE 3

Overall Effect of Various Cu (Oxide) Surface Species on the Autoxidation of Hexadecane Conditions: t = 100°C, 700 Torr O_2

Initial surface species	Effect on oxidation	Proposed mechanism for decomposition of t-BuO_2H
$Cu^+/O^{2-}[Cu_2O]$	Partial inhibition	Initially free-radical changes to mostly non-free-radical with time
$Cu^+/O^-[Cu(I)O]$	Partial inhibition	Initially free-radical changes to mostly non-free-radical with time
$Cu^{2+}/OH^-[Cu(OH)_2]$	Strong inhibition	Non-free-radical
$Cu^{2+}/O^{2-}[CuO]$	Strong acceleration	Free-radical

conversions and low initial hydroperoxide concentrations. A number of other contributing reactions also occur, but for the discussion here are reasonably regarded as unimportant.

$$RO_2H \rightarrow RO\cdot + HO\cdot \quad \text{initiation} \qquad (1)$$

$$\left.\begin{aligned} RO\cdot(HO\cdot) + RH &\rightarrow R\cdot + ROH(H_2O) \qquad (2)\\ R\cdot + O_2 &\rightarrow RO_2\cdot \qquad (3)\\ RO_2\cdot + RH &\rightarrow RO_2H + R\cdot \qquad (4)\end{aligned}\right\} \text{propagation}$$

$$2RO_2\cdot \rightarrow \text{nonradical products} \quad \text{termination} \qquad (5)$$

The major reaction products at temperatures around 100°C are usually alkyl hydroperoxides, and indeed these are observed under our present conditions (see Table 2, catalyst-free runs). The presence of a catalyst which decomposes hydroperoxides will markedly affect the rates of the initiation reactions and thus the course of the autoxidation. Several workers have proposed that the major effect of transition metal oxide catalysts on hydrocarbon autoxidation is alteration of the initiation reactions via surface-catalyzed hydroperoxide decompositions (*7*, *8*).

Based on our results with the carefully controlled surfaces generated from CO/prereduced copper and the results with pure CuO, we propose that the following types of reactions occur in hexadecane at 100°C for the surface species indicated. It is reasonably assumed that the hydroperoxides formed from hexadecane behave similarly, although the exact products formed will, of course, be different.

$$t\text{-}BuO_2H \xrightarrow{Cu^{2+}O^{2-}} \text{free radical products (e.g., } t\text{-}BuO\cdot, HO\cdot, t\text{-}BuO_2\cdot) \qquad (6)$$

$$t\text{-}BuO_2H \xrightarrow{Cu(OH)_2} \text{non-free-radical products [e.g., } t\text{-BuOH, } O_2, H_2O, (CH_3)_2CO, CH_3OH, CH_2{=}C(C\bar{H}_3)_2] \qquad (7)$$

The data do not provide us with information on the specific products formed, but reasonable guesses based on the known chemistry of hydroperoxides are given above (*20*). Thus, Reaction (6) followed by product desorption into solution provides a means for accelerating the initiation of autoxidation chains. On the other hand, Reaction (7) provides a means of trapping

and destroying hydroperoxides which are thus unable to contribute to radical production and chain initiation. If we consider a $Cu(OH)_2$ surface species, it would seem reasonable that the OH ligands would be exposed to the ambient side of the interface and thus control the chemistry of an absorbing group. Perhaps leading to proton or hydroxyl catalyzed heterolysis of the hydroperoxide. On the other hand, for a CuO surface species, interaction between the surface Cu^{2+} and an adsorbing hydroperoxide may be more likely without interfering HO ligands. Thus, typical electron transfer reactions might be expected. One fundamental study has been reported (*22*) on the kinetics of decomposition of *t*-butyl hydroperoxide vapor over a cuprous oxide surface between 110 and 170°C. Although an electron transfer mechanism was postulated, product studies were not performed and the exact surface species (probably Cu^{2+}) were not characterized.

The question of the effect of cuprous species on the decomposition of hydroperoxide is less clear. Both Cu_2O and Cu(I)O species give similar results, as shown in Fig. 8. A possible explanation for these observations is that the initial cuprous species are capable of limited free-radical production from adsorbed hydroperoxide

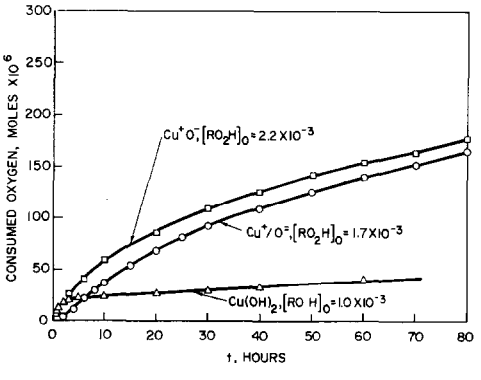

FIG. 8. Oxidation of hexadecane over copper oxide surfaces; □, Cu_2O surface, $[t\text{-}BuO_2H]_0 = 2.2 \times 10^{-3}$ *m*; ○, Cu_2O surface, $[t\text{-}BuO_2H]_0 = 1.67 \times 10^{-3}$ *m*; △, $Cu(OH)_2$ surface, $[t\text{-}BuO_2H]_0 = 1.04 \times 10^{-3}$ *m*.

decomposition, but these cuprous sites are unstable under the oxidizing conditions and are converted to cupric sites. Gradual formation of $Cu(OH)_2$ sites would cause increased trapping and thus result in decreasing oxidation rate. In Experiment 6–8, removal of the catalyst after 48 h and examination by X-ray photoelectron spectroscopy showed that an initial Cu_2O surface had been substantially converted to a $Cu(OH)_2$ species (see Section *Other Types of Copper Oxide Surfaces*). The hydroxyl groups required for the $Cu(OH)_2$ species could be provided directly from decomposition of the *t*-BuOOH and/or by H_2O, which is normally produced in an autoxidation via the hydrogen abstraction reactions of HO· radicals [Reaction (2)].

The phenomenon of dual catalysis-inhibition behavior of air-aged Cu metal can be understood in terms of the presence of both strong catalyzing and inhibiting sites on the catalyst surface combined with reversible adsorption. Preliminary attempts to quantitatively apply such a model using computational techniques, indicate that rapid switching is reasonable under our experimental conditions (*22*). Our experimental data suggest that the necessary combination of surface sites is present. The observed XPS spectrum (see Section *Standard Air-Aged Catalyst Runs*) is consistent with a surface mainly composed of Cu^{2+} and a mixture of O^{2-} and OH^-. The exposure of a fresh copper surface to air gradually produces a predominance of Cu^{2+} sites. The relative amount of the OH^- sites would be expected to vary as a function of the humidity of the air. When many of the cupric sites are removed by annealing at 280°C (see Table 1) the critical $[RO_2H]_0$ increases consistent with the appearance of a predominance of Cu^+ surface species. Exposure of the sample to H_2O/O_2 produces abundant $Cu(OH)_2$ sites also giving a high critical $[RO_2H]$ (Table 1). These are extremes of typical exposure conditions for freshly prepared cuprous oxide surfaces and

point out how such conditions may affect catalytic oxidation results. The Cu(air) sample used for the runs exhibits the critical concentration ranges shown in Fig. 6. Such a curve will be somewhat different for other samples aged and prepared independently, as several spot checks with other batches has shown.

At this point it is relevant to comment on the conflicting results of other workers. The discrepancy between Casemier and co-workers' (*4*) observation of the inertness of copper as a catalyst for cumene autoxidation at 90–100°C and Shalya and co-workers' (*5*) observation of significant catalytic effects in this same system may quite well be due to differing amounts of copper–oxygen surface species present in the catalysts of each study. It is not clear from the experimental details of the reports (*4*, *5*) what ultimate surface states were produced.

In this study we have been able to establish a correlation between catalytic activity and surface site structure with the implication that the chemistry is determined only by localized effects. It is important to point out that other factors, such as surface defects and semiconductor electronic properties, need to be evaluated before a detailed understanding of the surface mechanisms is known. Such factors as the thickness and nature of the intervening oxide phase(s) between the copper metal and the surface sites and the resultant electronic properties should be evaluated, and work is in progress to this end.

ACKNOWLEDGMENT

The authors acknowledge the helpful cooperation of F. Schrey in obtaining the surface area measurements.

REFERENCES

1. For example, see Voge, H. H., and Adams, C. R., *in* "Advances in Catalysis" (D. D. Eley, H. Pines, and P. B. Weisz, Eds.), Vol. 17, p. 151. Academic Press, New York, 1967.
2. Hansen, R. H., Russell, C. A., DeBenedictis, T., Martin, W. M., and Pascale, J. V., *J. Polym. Sci. (Part A)* **2**, 587 (1964).
3. Chan, M. G., and Allara, D. L., *J. Coll. Interface Sci.* **47**, 697 (1974).
4. Casemier, J. H. R., Niewenhuys, B. E., and Sachtler, W. M. H., *J. Catal.* **29**, 367 (1973).
5. Shalya, V. V. *et al.*, *Kinet. Catal.* **13**, 361 (English translation) (1972).
6. Poling, G. W., *J. Electrochem. Soc.* **117**, 520 (1970).
7. Mukherjee, A., and Graydon, W. F., *J. Phys. Chem.* **13**, 4232 (1967).
8. Gould, E. S., and Rado, M., *J. Catal.* **13**, 238 (1969).
9. Roberts, R. F., *J. Electron Spectrosc.* **4**, 273 (1974).
10. Robert, T., Bartel, M., and Offergeld, G., *Surf. Sci.* **33**, 123 (1972).
11. Hiatt, R., Mill, T., Irwin, K. C., and Castleman, J. K., *J. Org. Chem.* **33**, 1421 (1968).
12. Tompkins, H. G., and Allara, D. L., *J. Coll. Interface Sci.* **49**, 410 (1974).
13. Low, M. J. D., Brown, K. H., and Inoue, H. J., *J. Coll. Interface Sci.* **24**, 252 (1967).
14. Allara, D. L., Mill, T., Hendry, D. G., and Mayo, F. R., *Adv. Chem. Ser., No.* **76**, 40 (1968).
15. Mill, T., Mayo, F., Richardson, H., Irwin, K., and Allara, D. L., *J. Amer. Chem. Soc.* **94**, 6802 (1972).
16. Van Sickle, D., Mill, T., Mayo, F., Richardson, H., and Gould, C. W., *J. Org. Chem.* **38**, 4435 (1973).
17. Mill, T., and Montorsi, G., *Int. J. Chem. Kinetics* **5**, 119 (1973).
18. Allara, D. L., and Edelson, D., *Int. J. Chem. Kinet.* **4**, 345 (1972).
19. For a review, see Howard, J. A., *in* "Free Radicals" (J. Kochi, Ed.), Vol. II, Chap. 12. John Wiley and Sons, New York, 1973.
20. For example, see Hiatt, R. R., *in* "Organic Peroxides" (D. Swern, Ed.), Vol. II, Chap. 1. Wiley-Interscience, New York, 1971.
21. Hart, A. B., and Ross, R. A., *J. Catal.* **2**, 121 (1963).
22. Allara, D. L., and Edelson, D., to be published.